The Emerging Role of 3-Hydroxyanthranilic Acid on *C. elegans* Aging Immune Function

Luis S. Espejo[1], Destiny DeNicola[1], Leah M. Chang[1], Vanessa Hofschneider[1], Anne E. Haskins[1], Jonah Balsa[1], Samuel S. Freitas[1], Angelo Antenor[1], Sage Hamming[1], Bradford Hull[1], Raul Castro-Portuguez [1], Hope Dang[1], George L. Sutphin[1]

[1] Molecular & Cellular Biology, University of Arizona, Tucson, AZ, USA

Graphical Abstract

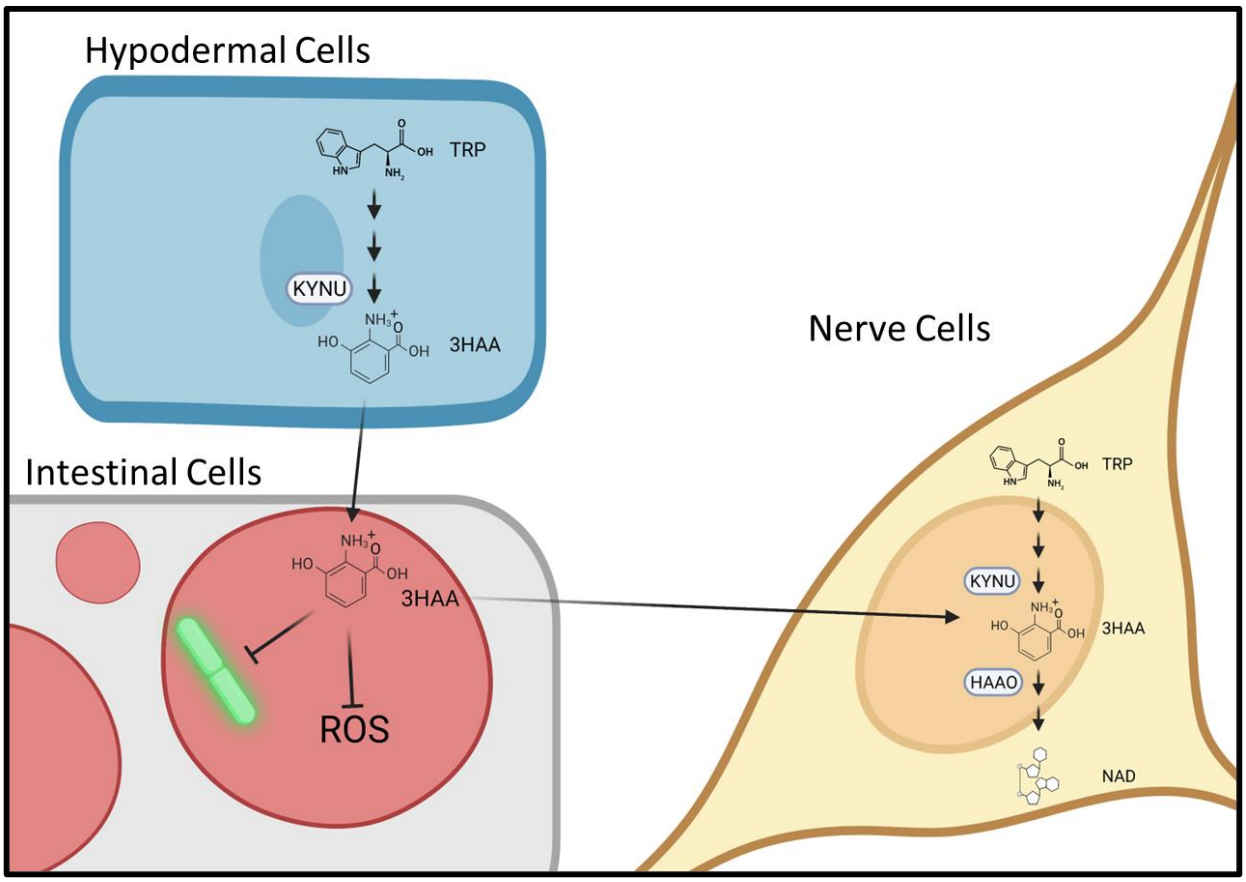

Abstract

3-hydroxyanthranilic acid (3HAA) is considered to be a fleeting metabolic intermediate along tryptophan catabolism through the kynurenine pathway. 3HAA and the rest of the kynurenine pathway have been linked to immune response in mammals yet whether it is detrimental or

advantageous is a point of contention. Recently we have shown that accumulation of this metabolite, either through supplementation or prevention of its degradation, extends healthy lifespan in *C. elegans* and mice, while the mechanism remained unknown. Utilizing *C. elegans* as a model we investigate how 3HAA and *haao-1* inhibition impact the host and the potential pathogens. What we find is that 3HAA improves host immune function with aging and serves as an antimicrobial against gram-negative bacteria. Regulation of 3HAA's antimicrobial activity is accomplished via tissue separation. 3HAA is synthesized in the *C. elegans* hypodermal tissue, localized to the site of pathogen interaction within the gut granules, and degraded in the neuronal cells. This tissue separation creates a new possible function for 3HAA that may give insight to a larger evolutionarily conserved function within the immune response.

Introduction

Caenorhabditis elegans has been a central model in diverse areas of age-related research since the 1980s[1], and has served as a model for innate immunity and host-pathogen interaction since the early 1990s.[2–4] *C. elegans* have a set number of somatic cells in adulthood but recapitulate aspects of molecular immune signaling which are orthologous to humans.[5–8] We previously found that accumulation of the tryptophan metabolite 3-hydroxyanthranilic acid (3HAA) via supplementation or inhibition of its metabolizing enzyme 3-hydroxyanthranilate 3,4-dioxygenase (HAAO) increases lifespan and extends many aspects of healthy aging in *C. elegans* and murine models.[9] 3HAA and other kynurenine pathway metabolites have been characterized as both pro-inflammatory and pro-immunogenic as well as anti-inflammatory and immunosuppressive.[10–21] A similar conflicting dichotomy is seen in the kynurenine pathway metabolites in regards to being pro-oxidant and antioxidant.[22–27] To evaluate therapeutic potential of 3HAA and kynurenine pathway manipulations, it is important to understand precisely what impact they have on aging immune health.

The dual natures of 3HAA argues for a context specific application of the metabolite, making the synthesis, localization, and degradation important factors in understanding the impact of the metabolite on immune function. For example the ability of 3HAA to be pro or anti-oxidant appears to be intricately linked to environmental factors like metal ions.[25] 3HAA has also been shown to reduce essential metal ions such as iron.[28] Our initial findings demonstrate that 3HAA

increases markers associated with anti-inflammatory responses as well as effectively neutralizes H2O2 in vitro.[9] These findings, among others, suggest an inhibitory role of 3HAA on inflammation and immune response but the overall impact on the immune function and the ability to combat pathogens during the aging process in undefined.[12]

Here we utilized *C. elegans* as a model to investigate the impact that elevated 3HAA has on aging immune function. Animals lacking *haao-1*, the gene encoding HAAO in *C. elegans*, are resistant to age-associated immune decline and better handle pathogenic challenge. *haao-1* mutants experienced lower rates of *Escherichia coli* infection and live longer once infected than their wild counterparts. Compared to the weaker pathogen *E. coli*, the kynurenine pathway is upregulated to a greater extent in response to the more pathogenic gram-negative *Pseudomonas aeruginosa.* In the absence of *haao-1* animals accumulate 3HAA with age, which may in turn be consumed in the defense against pathogens. The immune benefits of *haao-1* inhibition do not appear to operate through canonical *C. elegans* immune signaling pathway, but rather through direct antimicrobial activity of 3HAA itself, which is selectively localized to sites of pathogen interface within the intestinal enterocytes. This research provides a novel mechanistic role for 3HAA in *C. elegans* innate immune function and pathogen resistance.

Results

The kynurenine pathway catabolizes tryptophan(**Fig. 1A**) and is responsible for the majority of tryptophan metabolism in mammals.[29] It also is responsible for the biosynthesis of NAD+ contributing to the NAD+ pool along with dietary intake. We previously found that inhibition of *haao-1* extends lifespan in *C. elegans* mediated by physiological accumulation of the HAAO substrate 3HAA. The red 3HAA becomes visible under a dissection microscope by 11 days of age, or day 8 of adulthood (**Fig. 1B**)[9]. *C. elegans,* like mammals, experience a decline in immune function that results in increased susceptibility to pathogenic challenge with age.[30] Given the established role of kynurenine metabolism in immune function in mammals,[31,32] we asked whether kynurenine pathway interventions that alter lifespan would similarly impact immune function in *C. elegans* during aging. *C. elegans* with deletion mutations in four genes—*kmo-1*, *kynu-1*, *haao-1*, and *umps-1*—were raised on a live gram-negative *E. coli* food source (strain HT115, which are mildly pathogenic to *C. elegans*)[33] and challenged with the highly pathogenic gram-negative PA14 strain *P. aeruginosa* at the 4th larval stage (L4). Deletion of *kynu-1* and

74 *haao-1*, which encode kynureninase (KYNU) and HAAO, the enzymes are responsible for the
75 synthesis and degradation of 3HAA, respectively and are both long lived on *E. coli*[9,34] and
76 modestly resistant to PA14 challenge at L4 (**Fig. 1C**).

77 To investigate how *kynu-1* and *haao-1* impact *C. elegans* pathogen resistance during aging, *kynu-*
78 *1* and *haao-1* animals were raised on *E. coli* (strain OP50, which is slightly more pathogenic that
79 HT115) and challenged with PA14 at different ages (**Fig. 1D-H**). *kynu-1* knockout animals
80 displayed a decreased pathogen resistance during early adulthood (**Fig. 1G**). In contrast, *haao-1*
81 knockout animals had similar pathogen resistance to wild type during early adulthood, but were
82 more resistant than wild type when challenged at later ages (**Fig. 1I**). These results indicate that
83 *haao-1* deficient animals do not experience the same level age-associated immune decline or
84 *kynu-1* mutants.

85 *C. elegans* have several well-established immune signaling pathways. To test whether *haao-1*
86 inhibition improves immune response via these established pathways, epistasis survival
87 experiments were conducted (**Fig. 2A-C**). Lifespan extension via *haao-1* inhibition was not
88 rescued by *daf-16* (**Fig 2A**), *pmk-1* (**Fig 2B**), or *dbl-1* (**Fig. 2C**) RNAi, indicating that the age-
89 associated benefits form *haao-1* inhibition is likely not acting through classical *C. elegans*
90 immune signaling pathways. In *haao-1* deficient animals, 3HAA is consistently elevated relative
91 the wild type during aging. This elevation appears to modestly increase over time through day 4
92 of adulthood, and then increase dramatically between day 4 and 8 of adulthood (**Fig. 2D**). During
93 the aging process, the ratio of kynurenine (KYN) to tryptophan (TRP), a common measure of
94 kynurenine pathway activation that is used as a measure of IDO/TDO activity, decreases in wild
95 type, *kynu-1* and *haao-1* mutants (**Fig. 2E**). *kynu-1* mutants, and to a lesser extend *haao-1*
96 mutants, have a reduced KYN:TRP ratio throughout lifespan, which is likely due to elevated
97 KYN levels (**Fig. S3**) resulting from impaired KYN degradation, rather than higher activity of
98 TDO, as tryptophan is not reduced in these backgrounds (**Fig. S3**).

99 We next examined how kynurenine pathway metabolites change when wild type or *haao-1*
100 knockout worms are exposed to mildly pathogenic (*E. coli* strain OP50) vs. highly pathogenic (*P.*
101 *aeruginosa* strain PA14) bacteria. In wild type animals, the KYN:TRP ratio increases following
102 exposure to PA14, driven by a decrease in TRP and an increase in KYN (Fig. S2), suggesting
103 activation of TDO-2 to increase flux through the kynurenine pathway (**Fig. 2H**). This indicates

104 that *C. elegans* promote kynurenine pathway flux via activation of TDO-2 in the presence of
105 strong pathogens, paralleling IDO activation in mammals.[35] The opposite relationship is seen in
106 the *haao-1* mutants, with the KYN:TRP ratio elevated relative to wild type animals on *E. coli*,
107 but strongly repressed following PA14 challenge (**Fig. 2H**). This flip in KYN/TRP in *haao-1*
108 mutants is likely due to *haao-1* mutants accumulating KYN in low pathogen environments,
109 potentially due to feedback inhibition of KYNU, but tryptophan levels follow the same trend as
110 wild type animals (**Supplemental Fig. 2**). Additionally, there is a trend toward increased in 3-
111 hydroxykynurenine (3HK), the metabolite that is converted to 3HAA by KYNU (**Fig. 1A**), in
112 wild type animals under strong pathogenic challenge (**Fig. 2I**) suggesting an increased flow
113 towards 3HAA during challenge. When animals age on the standard OP50 diet 3HK levels
114 decrease over time (**Fig. 2F**). While 3HAA itself decreases in response to PA14 challenge (**Fig.
115 2G**), the ratio of the oxidized product of 3HAA, cinnabarinic acid (CA), to 3HAA increases **(Fig.
116 2J**) indicating potential consumption of 3HAA in defense against strong pathogens. Taken
117 together, this evidence suggests the kynurenine pathway is upregulated under strong pathogenic
118 challenge and that 3HAA is consumed in the process of host defense.

119 To understand how *haao-1* inhibition and 3HAA impact the host-pathogen relationship, we
120 examined the impact *haao-1* deletion on the dynamics of bacterial infection using a new system
121 that we recently developed called Systematic Imaging of *Caenorhabditis* Killing Organisms
122 (SICKO)[36]. SICKO allows several metrics of infection with fluorescently-labeled bacteria to be
123 monitored over time in individual free-crawling *C. elegans*[36], including infection initiation,
124 progression, and subsequent survival. We exposed wild type and *haao-1* knockout worms to *E.*
125 *coli* OP50 constitutive expressing GFP for 7 days, transferred randomly selected animals to
126 single worm culture environments[37], and monitored subsequent infection dynamics and survival
127 over time. Both *haao-1* mutants and wild type animals experienced death associated with
128 infection, but *haao-1* mutants experience a decreased rate of infection and infection associated
129 death (**Fig. 3A**). Additionally, wild animals experienced an increase onset of infection post
130 challenge (**Fig 3B**). Infected *haao-1* knockout animals performed significantly worse than their
131 non-infected counterparts indicating toxicity of GOP50 is less impactful than infection in relation
132 to death. Once infected, *haao-1* animals have improved survival relative to wild type (**Fig. 3C**).
133 SICKO calculates a infection index (aka the SICKO Score) that incorporates information about
134 current level of infection in live animals and the number of past deaths in infected animals,

135 providing a composite measure of infection severity that can be used to compare populations
136 with distinct survival and infection dynamics over time[36]. *haao-1* mutants experienced lower
137 infection index relative to wild type animals throughout life (**Fig. 3D**).

138 These findings indicate that HAAO inhibition is sufficient to improve host response to
139 pathogens in terms of resistance to both infection initiation and progression. Because 3HAA is
140 elevated in *haao-1* knockout animals, is consumed during PA14 infection, and mimics lifespan
141 extension from *haao-1* knockdown, and because lifespan extension from *haao-1* knockout is not
142 dependent on canonical immune pathways, we next asked whether 3HAA might media the
143 improved pathogen resistance of *haao-1* deficient animals by directly impacting bacteria survival
144 and growth. In both GOP50 and GPA14 cultured in liquid media, 3HAA inhibited bacterial
145 growth in a dose-dependent manner (**Fig. 3E-F**). Different aspects of bacterial growth dynamics
146 can be quantified from the bacterial growth curves; V-max provides insight to maximum growth
147 rate of the bacteria within the medium, while lag time is a reflection of the size of the initial
148 population and is thus an indication of initial impact of an intervention on bacterial death. 3HAA
149 inhibits the GOP50 V-max in a dose-dependent manner (**Fig. 3G**). Here we found that both
150 pathogen lagtimes directly correlate to bacteria concentration (Supplemental Fig. 4). The lagtime
151 for both the weak and strong gram-negative pathogens is significantly impacted by 3HAA in a
152 dose dependent manner (**Fig. 3I**) indicating 3HAA prevents initiation of bacterial growth in early
153 stages or kills a subset of the bacteria on first exposure.

154 To understand what context 3HAA may potentially contact pathogens it is critical to pinpoint its
155 location, site of synthesis, and site of degradation. Early in adulthood animals display a distinct
156 separation of 3HAA synthesis and degradation (**Fig. 4A-B**). Synthesis of 3HAA via KYNU-1
157 appears to happen across many tissues of the animal and heavily in the hypodermis. While
158 degradation via HAAO-1 only occurs in a small subsection of tissue in which synthesis occurs.
159 HAAO-1 during early adulthood primarily is located within the neurons (Supplemental Fig. 5).
160 Surprisingly, this special temporal separation of synthesis and degradation becomes lost as the
161 animal passes 6 days of adulthood (**Fig. 4B**). This special temporal gap creates a expands the
162 potential localization of 3HAA between the process of metabolism through the kynurenine
163 pathway.

164 Upon further inspection of 3HAA accumulation in haao-1 mutants, 3HAA appears not to be at
165 the site of synthesis or degradation but rather located in gut granule structures within the *C.*
166 *elegans* intestine (**Fig. 4C**). Due to the green pigmentation of PA14 toxins (Supplemental Fig. 5)
167 animals challenged with the pathogen can also be observed with remnants of the pathogen in
168 similar gut granular structures. Additionally, *haao-1* mutants challenged with PA14 have no
169 distinctly separate green or red granular structures, indicating that 3HAA may contact pathogens
170 within the subcellular structure. This finding potentially uncovers a previously unknown immune
171 role and regulation of 3HAA in *C. elegans* pathogen combat. To distinguish if the 3HAA in the
172 gut granules is from a distal tissue a *rde-1*, required for RNAi impact, mutant selectively
173 functional in the hypodermis was utilized. Indeed, when kynu-1 is inhibited in the hypodermis,
174 significant amounts of 3HAA fail to accumulate in the gut granules (**Fig. 4D**). Taken together
175 this demonstrates that 3HAA is synthesized in a distal tissue and is transported to the pathogen
176 interface.

177 The *C. elegans* gut granules have been proposed to be heavily regulated in regard to metal ion
178 availability. 3HAA is also known to interact with iron leaving the potential of synergistic
179 interactions in vivo. To test this possibility 3HAA was combined with iron perturbations to assess
180 solid surface growth of pathogens. A strong synergistic impact is seen between 3HAA and the
181 iron chelator deferoxamine (DFO) (**Fig. 4E**). DFO on it's own does not have a strong impact on
182 bacterial growth in solid or liquid culture (Supplemental Fig. 6). Not only I does the combination
183 of DFO and 3HAA inhibit bacterial ability to form colonies, the colonies capable of growing are
184 significantly smaller than control colonies, or DFO and 3HAA alone (**Fig. 4F-G**). 1mM 3HAA
185 by itself does not significantly impact bacterial growth but combined with likely metal
186 perturbations in gut granules accounts for a potent antimicrobial activity of a conserved immune
187 response in *C. elegans*.

188

189 **Discussion**

190 The kynurenine is evolutionarily conserved and has been tied to immune function in mammals
191 with contradictory indications to its role. We previously demonstrated that *haao-1* inhibition and
192 3HAA supplementation was capable of extending healthy lifespan in *C. elegans* and mice. Here
193 we see that kynurenine pathway activity is linked to *C. elegans* immune function. In particular

194 *haao-1* inhibition and 3HAA serve to decrease age-associated immune decline and help the host
195 combat pathogen. The pathway is activated in response to strong pathogenic challenge and flux
196 is funneled toward the production of 3HAA which is consumed in the process of combating
197 pathogen. *haao-1* animals also performed better under pathogenic challenge. They survived
198 stronger pathogenic challenges with age in addition to fending off weaker pathogenic challenges
199 and slowing the progression of infection throughout the population.

200 Surprisingly, it does not appear that *haao-1* effects on *C. elegans* immune function occur through
201 the canonical *C. elegans* immune signaling pathways. It appears that the major activity of 3HAA
202 occurs on the pathogen itself. This activity is regulated by localization of 3HAA to the gut cell
203 epithelium. It seems likely that the 3HAA resides in the gut granules because another kynurenine
204 metabolite, anthranilic acid, is also present in that same sub cellular structure.[38,39] In the gut
205 granules, when 3HAA comes into contact with pathogens its antimicrobial activity would may
206 serve as a host defense against invading pathogens. Regulation of antimicrobial activity is only
207 possible via tissue separation in synthesis and degradation. By being synthesized in the
208 hypodermis, localized in the gut granules, and degraded in the neurons, 3HAA can reach higher
209 concentrations than if it was distributed throughout the body. This may explain why 3HAA has
210 been viewed as a fleeting metabolic intermediate in the past; as if one only looks at sites where it
211 is manufactured or degraded the 3HAA itself may not be in abundant levels. Additionally,
212 antimicrobial affects of 3HAA may be intricately linked to metal ion availability. 3HAA has been
213 noted to interact with ions in the past acting as a reducing agent. This would not be the first
214 account of intermediate function as 3HAA has been proposed as a microbial attack mechanism in
215 conjunction with iron sequestration in *Cryptococcus neoformans* and other organisms.[40,41]
216 Because elevated 3HAA and kynurenine pathway activity has been witnessed in patients
217 undergoing immune challenge this research may provide insight into 3HAA's evolutionary role
218 in immune function. 3HAA's elevation may due to immune response mounting against potential
219 pathogens. This impact of 3HAA may also be context specific. In one tissue it may combat
220 pathogens while in another may assist in oxidative stress. This creates multiple benefits that all
221 may stem from the conserved metabolite.

222

223

224 **References**

225 1. Johnson, T. E. & Wood, W. B. Genetic analysis of life-span in Caenorhabditis elegans.
226 *Proc. Natl. Acad. Sci. U. S. A.* **79**, 6603–6607 (1982).

227 2. Pukkila-Worley, R. & Ausubel, F. M. Immune defense mechanisms in the Caenorhabditis
228 elegans intestinal epithelium. *Curr. Opin. Immunol.* **24**, 3–9 (2012).

229 3. Taffoni, C. & Pujol, N. Mechanisms of innate immunity in C. elegans epidermis. *Tissue*
230 *Barriers* **3**, e1078432 (2015).

231 4. Pujol, N. *et al.* Distinct innate immune responses to infection and wounding in the C.
232 elegans epidermis. *Curr. Biol. CB* **18**, 481–489 (2008).

233 5. Kurz, C. L. & Tan, M.-W. Regulation of aging and innate immunity in C. elegans. *Aging*
234 *Cell* **3**, 185–193 (2004).

235 6. Marsh, E. K. & May, R. C. Caenorhabditis elegans, a Model Organism for Investigating
236 Immunity. *Appl. Environ. Microbiol.* **78**, 2075–2081 (2012).

237 7. Arras, L. D. *et al.* An Evolutionarily Conserved Innate Immunity Protein Interaction
238 Network. *J. Biol. Chem.* **288**, 1967–1978 (2013).

239 8. Elkabti, A. B., Issi, L. & Rao, R. P. Caenorhabditis elegans as a Model Host to Monitor
240 the Candida Infection Processes. *J. Fungi* **4**, (2018).

241 9. Dang, H. *et al.* 3-hydroxyanthranilic acid – a new metabolite for healthy lifespan
242 extension. 2021.06.01.446651 Preprint at https://doi.org/10.1101/2021.06.01.446651 (2021).

243 10. Lowe, M. M. *et al.* Identification of Cinnabarinic Acid as a Novel Endogenous Aryl
244 Hydrocarbon Receptor Ligand That Drives IL-22 Production. *PLoS ONE* **9**, e87877 (2014).

245 11. Hoshi, M. *et al.* 3-Hydroxykynurenine Regulates Lipopolysaccharide-Stimulated IL-6
246 Production and Protects against Endotoxic Shock in Mice. *ImmunoHorizons* **5**, 523–534 (2021).

247 12. Christen, S., Thomas, S. R., Garner, B. & Stocker, R. Inhibition by interferon-gamma of
248 human mononuclear cell-mediated low density lipoprotein oxidation. Participation of tryptophan
249 metabolism along the kynurenine pathway. *J. Clin. Invest.* **93**, 2149–2158 (1994).

250 13. Liu, X., Newton, R. C., Friedman, S. M. & Scherle, P. A. Indoleamine 2,3-dioxygenase,
251 an emerging target for anti-cancer therapy. *Curr. Cancer Drug Targets* **9**, 938–952 (2009).

252 14. Sekine, H. *et al.* Hypersensitivity of Aryl Hydrocarbon Receptor-Deficient Mice to
253 Lipopolysaccharide-Induced Septic Shock. *Mol. Cell. Biol.* **29**, 6391–6400 (2009).

254 15. Huttunen, R. *et al.* HIGH ACTIVITY OF INDOLEAMINE 2,3 DIOXYGENASE
255 ENZYME PREDICTS DISEASE SEVERITY AND CASE FATALITY IN BACTEREMIC
256 PATIENTS. *Shock* **33**, 149 (2010).

257 16. Tattevin, P. *et al.* Enhanced Indoleamine 2,3-Dioxygenase Activity in Patients with
258 Severe Sepsis and Septic Shock. *J. Infect. Dis.* **201**, 956–966 (2010).

259 17. Wirthgen, E. & Hoeflich, A. Endotoxin-Induced Tryptophan Degradation along the
260 Kynurenine Pathway: The Role of Indolamine 2,3-Dioxygenase and Aryl Hydrocarbon Receptor-
261 Mediated Immunosuppressive Effects in Endotoxin Tolerance and Cancer and Its Implications
262 for Immunoparalysis. *J. Amino Acids* **2015**, (2015).

263 18. Litzenburger, U. M. *et al.* Constitutive IDO expression in human cancer is sustained by
264 an autocrine signaling loop involving IL-6, STAT3 and the AHR. *Oncotarget* **5**, 1038–1051
265 (2014).

266 19. Jung, I. D. *et al.* Blockade of Indoleamine 2,3-Dioxygenase Protects Mice against
267 Lipopolysaccharide-Induced Endotoxin Shock. *J. Immunol.* **182**, 3146–3154 (2009).

268 20. Mondanelli, G. *et al.* A Relay Pathway between Arginine and Tryptophan Metabolism
269 Confers Immunosuppressive Properties on Dendritic Cells. *Immunity* **46**, 233–244 (2017).

270 21. Hayashi, T. *et al.* 3-Hydroxyanthranilic acid inhibits PDK1 activation and suppresses
271 experimental asthma by inducing T cell apoptosis. *Proc. Natl. Acad. Sci.* **104**, 18619–18624
272 (2007).

273 22. Mor, A., Tankiewicz-Kwedlo, A., Krupa, A. & Pawlak, D. Role of Kynurenine Pathway
274 in Oxidative Stress during Neurodegenerative Disorders. *Cells* **10**, 1603 (2021).

275 23. Taniguchi, T. *et al.* Indoleamine 2,3-dioxygenase. Kinetic studies on the binding of
276 superoxide anion and molecular oxygen to enzyme. *J. Biol. Chem.* **254**, 3288–3294 (1979).

277 24. Grant, R. S., Naif, H., Espinosa, M. & Kapoor, V. IDO induction in IFN-gamma activated
278 astroglia: a role in improving cell viability during oxidative stress. *Redox Rep. Commun. Free*
279 *Radic. Res.* **5**, 101–104 (2000).

280 25. Goldstein, L. E. *et al.* 3-Hydroxykynurenine and 3-Hydroxyanthranilic Acid Generate
281 Hydrogen Peroxide and Promote α-Crystallin Cross-Linking by Metal Ion Reduction.
282 *Biochemistry* **39**, 7266–7275 (2000).

283 26. Pérez-González, A., Alvarez-Idaboy, J. R. & Galano, A. Dual antioxidant/pro-oxidant
284 behavior of the tryptophan metabolite 3-hydroxyanthranilic acid: a theoretical investigation of
285 reaction mechanisms and kinetics. *New J. Chem.* **41**, 3829–3845 (2017).

286 27. Darlington, L. G. *et al.* On the Biological Importance of the 3-hydroxyanthranilic Acid:
287 Anthranilic Acid Ratio. *Int. J. Tryptophan Res. IJTR* **3**, 51–59 (2010).

288 28. Nyhus, K. J., Wilborn, A. T. & Jacobson, E. S. Ferric iron reduction by Cryptococcus
289 neoformans. *Infect. Immun.* **65**, 434–438 (1997).

290 29. King, N. J. C. & Thomas, S. R. Molecules in focus: Indoleamine 2,3-dioxygenase. *Int. J.*
291 *Biochem. Cell Biol.* **39**, 2167–2172 (2007).

30. Kim, S. S., Sohn, J. & Lee, S.-J. V. Immunosenescence in Caenorhabditis elegans. *Immun. Ageing* **19**, 56 (2022).

31. Mándi, Y. & Vécsei, L. The kynurenine system and immunoregulation. *J. Neural Transm.* **119**, 197–209 (2012).

32. Cribbs, A. P. & Williams, R. O. Role of the Kynurenine Pathway in Immune-Mediated Inflammation. in *Targeting the Broadly Pathogenic Kynurenine Pathway* (ed. Mittal, S.) 93–107 (Springer International Publishing, 2015). doi:10.1007/978-3-319-11870-3_7.

33. Stuhr, N. L. & Curran, S. P. Bacterial diets differentially alter lifespan and healthspan trajectories in C. elegans. *Commun. Biol.* **3**, 1–18 (2020).

34. Sutphin, G. L. *et al.* Caenorhabditis elegans orthologs of human genes differentially expressed with age are enriched for determinants of longevity. *Aging Cell* **16**, 672–682 (2017).

35. Badawy, A. A.-B. & Guillemin, G. The Plasma [Kynurenine]/[Tryptophan] Ratio and Indoleamine 2,3-Dioxygenase: Time for Appraisal. *Int. J. Tryptophan Res. IJTR* **12**, 1178646919868978 (2019).

36. Espejo, L. S. *et al.* SICKO: Systematic Imaging of Caenorhabditis Killing Organisms. 2023.02.17.529009 Preprint at https://doi.org/10.1101/2023.02.17.529009 (2023).

37. Espejo, L. *et al.* Long-Term Culture of Individual Caenorhabditis elegans on Solid Media for Longitudinal Fluorescence Monitoring and Aversive Interventions. *J. Vis. Exp. JoVE* (2022) doi:10.3791/64682.

38. Coburn, C. & Gems, D. The mysterious case of the C. elegans gut granule: death fluorescence, anthranilic acid and the kynurenine pathway. *Front. Genet.* **4**, 151 (2013).

39. Coburn, C. *et al.* Anthranilate Fluorescence Marks a Calcium-Propagated Necrotic Wave That Promotes Organismal Death in C. elegans. *PLOS Biol.* **11**, e1001613 (2013).

40. Jung, W. H. & Kronstad, J. W. Iron and fungal pathogenesis: a case study with Cryptococcus neoformans. *Cell. Microbiol.* **10**, 277–284 (2008).

41. Zhang, Y., Wang, F. & Zhao, Z. Metabonomics reveals that entomopathogenic nematodes mediate tryptophan metabolites that kill host insects. *Front. Microbiol.* **13**, (2022).

Graphical Abstract

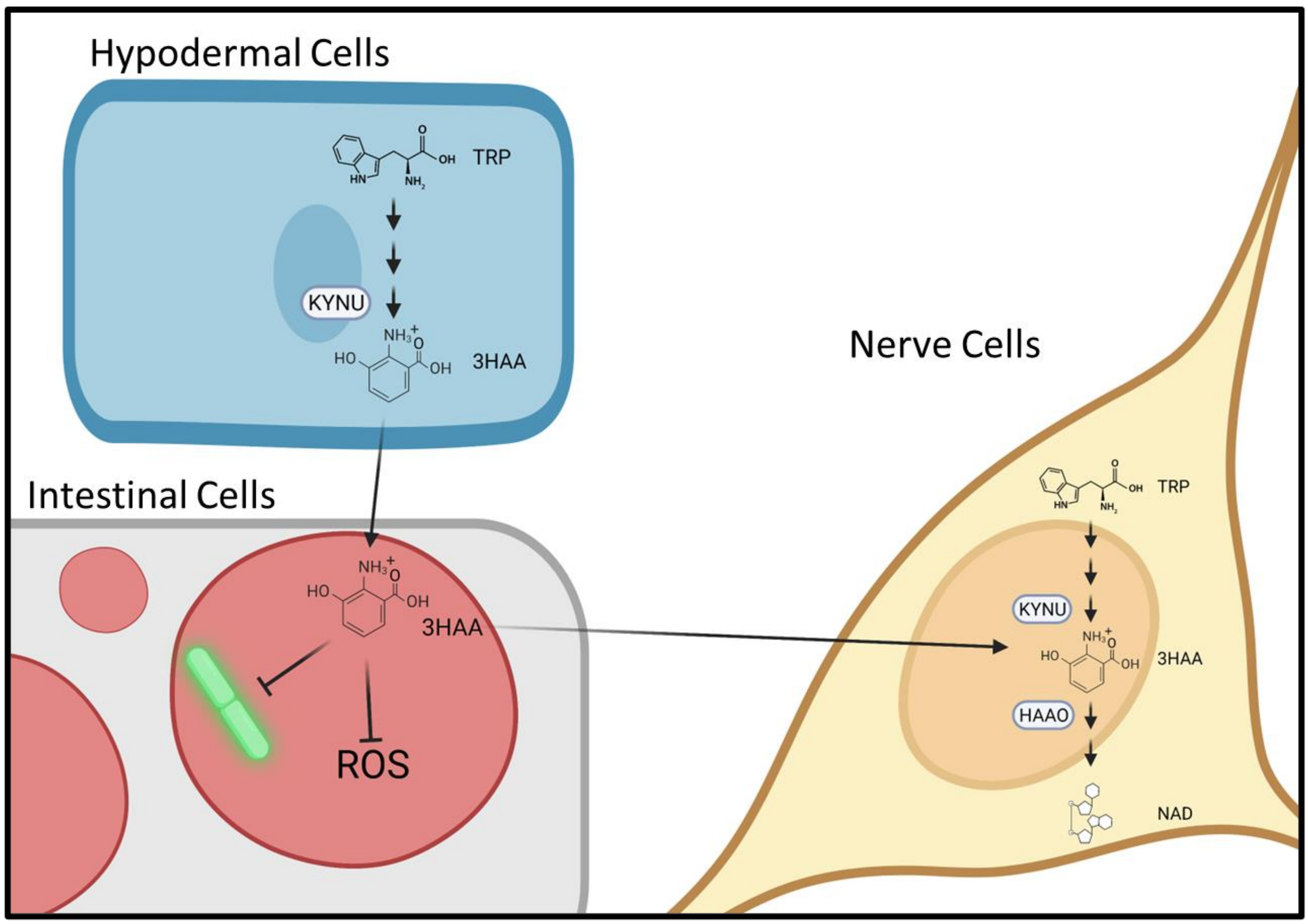

Figure 1: *haao-1* Mutants Resistant to Age-Associated Immune Decline.

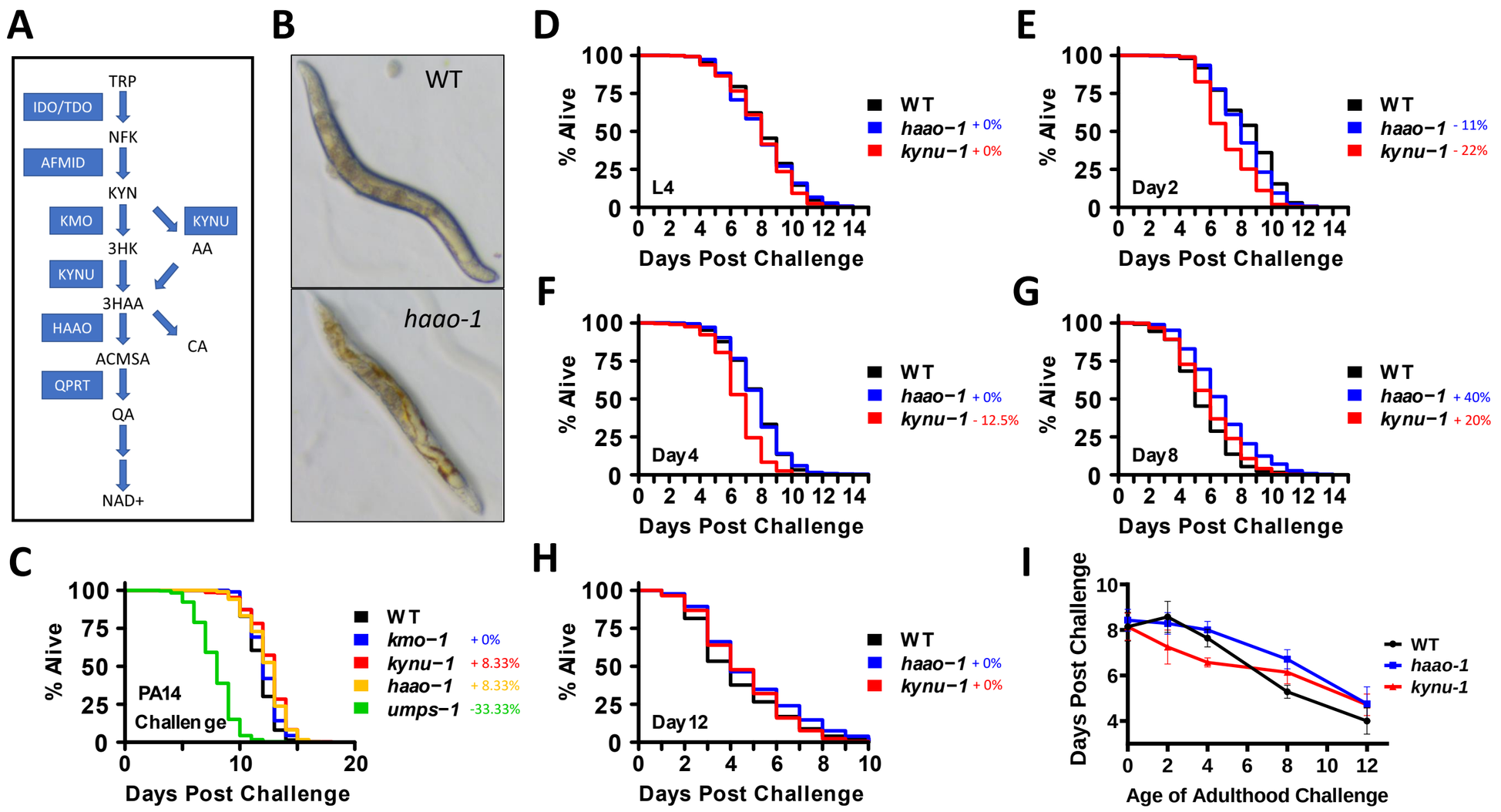

(A) The kynurenine pathway is responsible for a majority of the metabolism of tryptophan and the endogenous production of NAD+. **(B)** *haao-1* mutants grow visibly red with age due to the accumulation of the 3HAA metabolite. **(C)** Kynurenine pathway mutants synchronized on HT115 EV RNAi differentially impact host survival upon *P. aeruginosa* challenge at L4 stage. **(D)** Survival of haao-1 and kynu-1 mutants synchronized on OP50 challenge with *P. aeruginosa* at L4 stage. **(E-H)** C. elegans survival reared on OP50 bacteria then challenged with *P. aeruginosa* at days: 2, 4, 8, and 12 of adulthood. **(I)** Characterization of age-associated immune decline measuring median survival post *P. aeruginosa* challenge.

Fig 2 Immune genes and Metabolic Activity

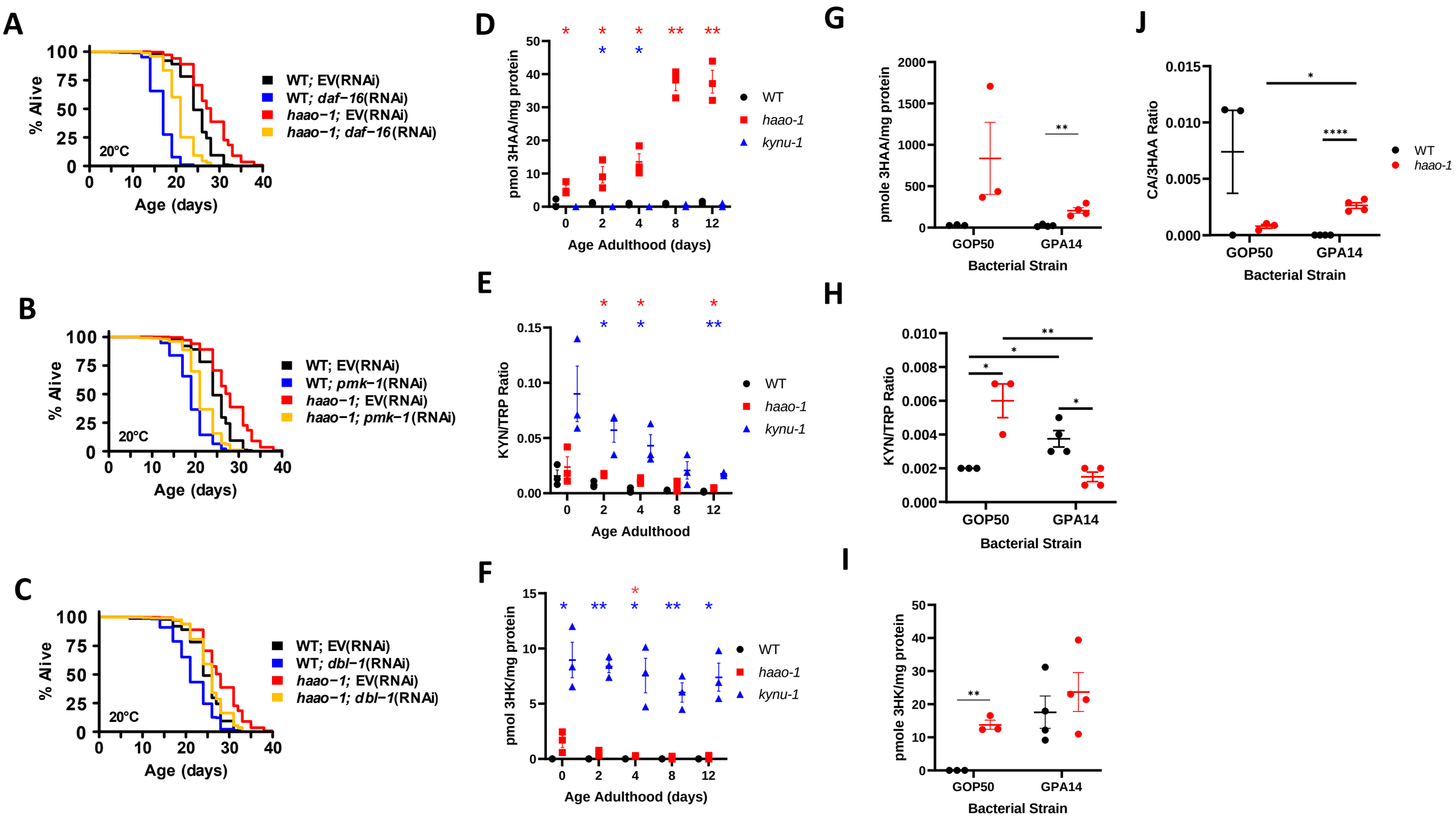

Figure 2. haao-1 Mutant Improved Immune Function is Independent of Classical C. elegans Immune Signaling Funneling Pathway Flux Towards 3HAA. (A) Epistatic survival of *haao-1* mutants using *daf-16* HT115 knock down. **(B)** Epistatic survival of *haao-1* mutants using *pmk-1* HT115 knock down. **(C)** Epistatic survival of haao-1 mutants using *dbl-1* HTT115 knock down. **(D)** Mass spectrometry of 3HAA metabolite over course of aging normalized to total population protein. **(E)** KYN/TRP ratio throughout aging up to day 12 of adulthood, classically used to represent flux through the kynurenine pathway. **(F)** Mass spectrometry of 3HK metabolite throughout aging normalized to total population protein. **(G)** Mass spectrometry of 3HAA metabolite of *haao-1* mutants and WT animals under low and high pathogenic conditions of GOP50 and GPA14. **(H)** KYN/TRP ratio of *haao-1* and WT under different pathogenic challenges obtained via mass spectrometry. **(I)** Mass spectrometry of 3HK metabolite in *haao-1* and WT under different pathogenic challenges. **(J)** CA/3HAA metabolite ratio determined via mass spec representing oxidation of 3HAA to CA.

Figure 3 SICKO and Bacteria Response to 3HAA

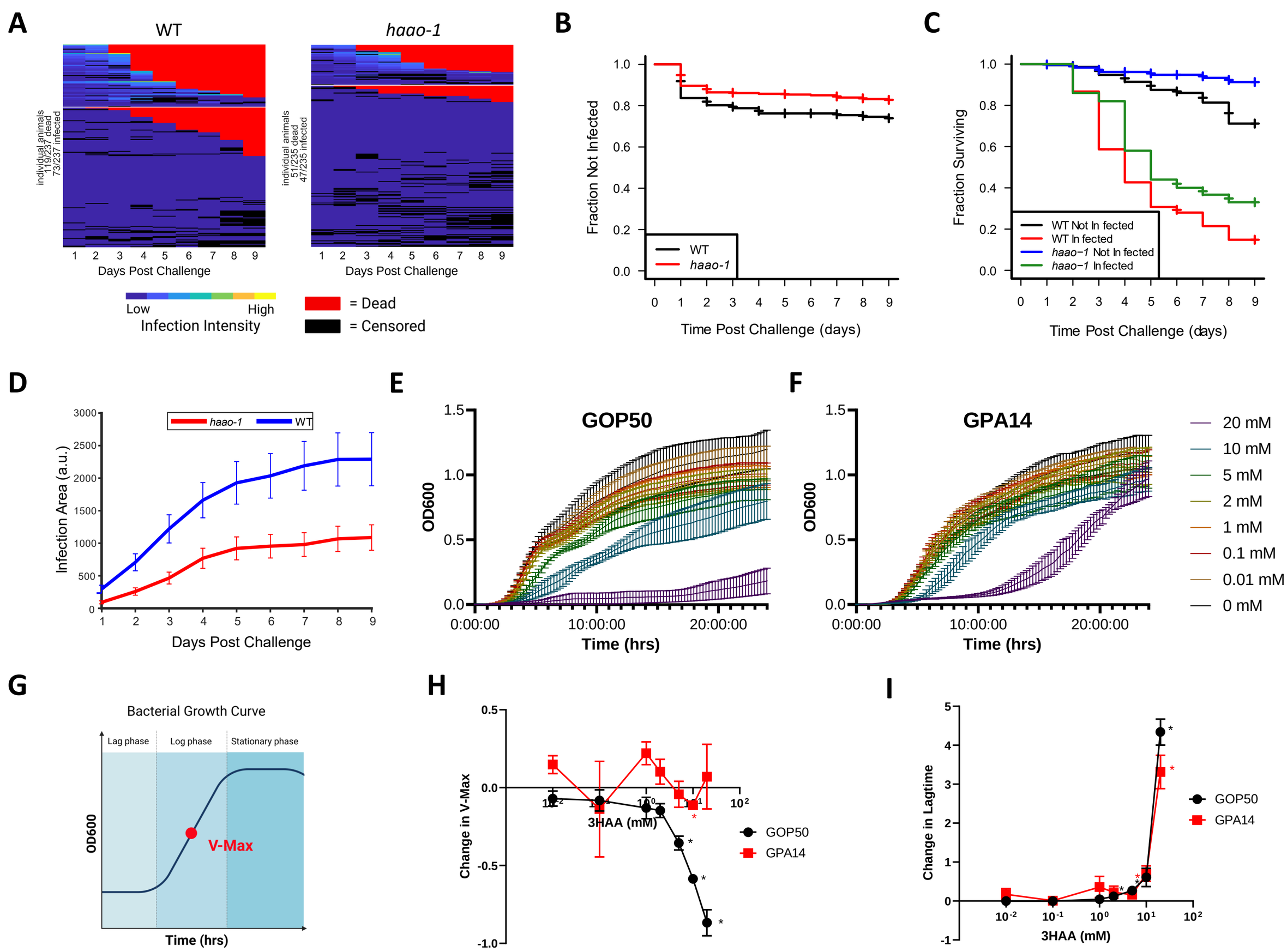

Figure 3. *haao-1* Mutants have Improved Response to Pathogens while the Accumulating 3HAA has Strong Antimicrobial Activity. (A) SICKO (Systematic Imaging of *Caenorhabditis* Killing Organisms) infection tracking of GOP50 infection area in WT and *haao-1* animals after 7-day pathogenic challenge. All animals above the white line are infected in each condition. WT animals were significantly more associated with infection ($p < 0.005$; chi-squre). In both genetic backgrounds death was associated with infection ($p < 0.05$; chi-square). **(B)** Onset of detectable infections in WT and *haao-1* animals using SICKO system following pathogenic challenge. *haao-1* animals had significantly different onset of infection ($p < 0.05$, log-rank test). (C) Survival

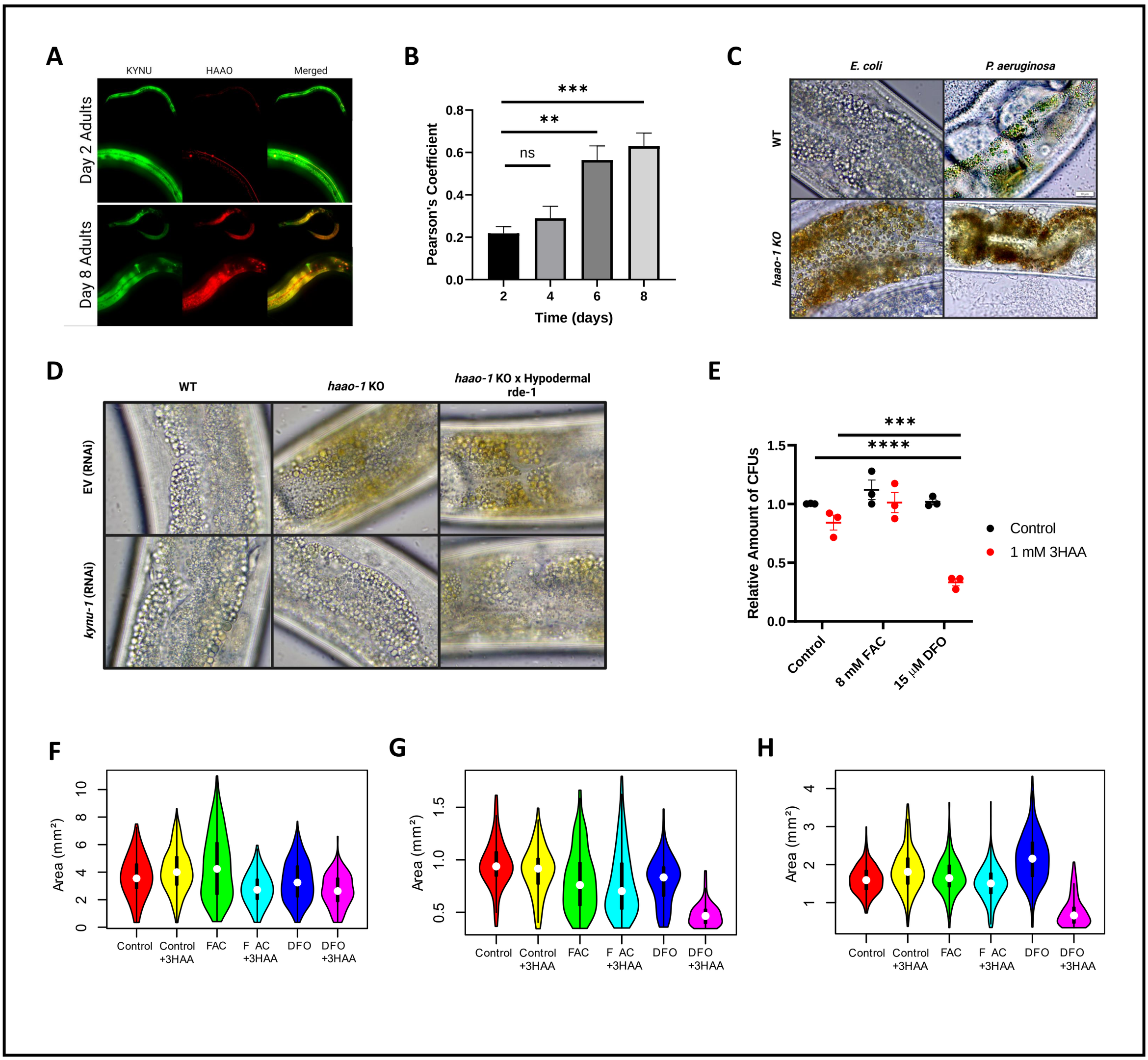
A
KYNU
HAAO
Merged
Day 2 Adults
Day 8 Adults
B
***
**
ns
Pearson's Coefficient
0.8
0.6
0.4
0.2
0.0
2
4
6
8
Time (days)
C
E. coli
P. aeruginosa
WT
haao-1 KO
D
WT
haao-1 KO
haao-1 KO x Hypodermal rde-1
EV (RNAi)
kynu-1 (RNAi)
E
***
****
Relative Amount of CFUs
1.5
1.0
0.5
0.0
Control
8 mM FAC
15 μM DFO
Control
1 mM 3HAA
F
Area (mm²)
0
2
4
6
8
10
Control
Control +3HAA
FAC
F AC +3HAA
DFO
DFO +3HAA
G
Area (mm²)
0.5
1.0
1.5
Control
Control +3HAA
FAC
F AC +3HAA
DFO
DFO +3HAA
H
Area (mm²)
1
2
3
4
Control
Control +3HAA
FAC
F AC +3HAA
DFO
DFO +3HAA